

Molecular Cloning and Characterization of Phospholipase C Zeta in Equine Sperm and Testis Reveals Species-Specific Differences in Expression of Catalytically Active Protein¹

S.J. Bedford-Guaus,^{2,3} L.A. McPartlin,³ J. Xie,⁴ S.L. Westmiller,³ M.G. Buffone,⁵ and M.S. Roberson⁴

Departments of Clinical Sciences³ and Biological and Biomedical Sciences,⁴ College of Veterinary Medicine, Cornell University, Ithaca, New York
Instituto de Biología y Medicina Experimental,⁵ National Research Council of Argentina (CONICET), Buenos Aires, Argentina

ABSTRACT

Oocyte activation at fertilization is brought about by the testis-specific phospholipase C zeta (PLCZ), owing to its ability to induce oscillations in intracellular Ca^{2+} concentration ($[\text{Ca}^{2+}]_i$). Whereas this is a highly conserved mechanism among mammals, important species-specific differences in PLCZ sequence, activity, and expression have been reported. Thus, the objectives of this research were to clone and characterize the intracellular Ca^{2+} -releasing activity and expression of equine PLCZ in sperm and testis. Molecular cloning of equine PLCZ yielded a 1914-bp sequence that translated into a protein of the appropriate size (~73 kDa), as detected with an anti-PLCZ-specific antibody. Microinjection of 1 $\mu\text{g}/\mu\text{l}$ of equine PLCZ cRNA supported $[\text{Ca}^{2+}]_i$ oscillations in murine oocytes that were of a higher relative frequency than those generated by an equivalent concentration of murine *Plcz* cRNA. Immunofluorescence revealed expression of PLCZ over the acrosome, equatorial segment, and head-midpiece junction; unexpectedly, PLCZ also localized to the principal piece of the flagellum in all epididymal, uncapacitated, and capacitated sperm. Immunostaining over the acrosome was abrogated after induction of acrosomal exocytosis. Moreover, injection of either sperm heads or tails into mouse oocytes showed that PLCZ in both fractions is catalytically active. Immunohistochemistry on equine testis revealed expression as early as the round spermatid stage, and injection of these cells supported $[\text{Ca}^{2+}]_i$ oscillations in oocytes. In summary, we report that equine PLCZ displays higher intrinsic intracellular Ca^{2+} -releasing activity than murine PLCZ and that catalytically active protein is expressed in round spermatids as well as the sperm flagellum, emphasizing important species-specific differences. Moreover, some of these results may suggest potential novel roles for PLCZ in sperm physiology.

calcium, oocyte activation, phospholipase C zeta, stallion

INTRODUCTION

Oocyte activation at fertilization encompasses the release from metaphase II (MII) arrest, prevention of polyspermy, pronuclear formation, and initiation of embryonic cleavage (for reviews, see [1, 2]). In all mammalian species studied, this is brought about by repetitive increases in intracytoplasmic Ca^{2+} concentration ($[\text{Ca}^{2+}]_i$) [3–7], referred to as $[\text{Ca}^{2+}]_i$ oscillations. Present evidence suggests that the factor responsible for the initiation of these $[\text{Ca}^{2+}]_i$ oscillations is a testis-specific isoform of phospholipase C (PLC), PLC zeta (PLCZ), which is delivered by the sperm at the time of fertilization [8]. The identity of this protein as a PLC accounts for the findings that cleavage of phosphatidylinositol 4,5-bisphosphate (PIP_2) and production of 1,4,5-inositol trisphosphate within the oocyte are required for the initiation and maintenance of the $[\text{Ca}^{2+}]_i$ oscillations observed at fertilization [9–12]. PLCZ was first cloned from mouse testis [8] and has since been sequenced in the human, monkey [13], chicken [14], pig [15], medaka fish, rat [16], and hamster [17], owing to a highly conserved mechanism for triggering egg activation in mammals and, potentially, other vertebrate species.

Similar in structure to other PLC isoforms, PLCZ spans four EF hand domains at the N terminus, X and Y catalytic domains, and a C2 terminus domain; however, PLCZ lacks the N-terminal plextrin-homology (PH) domain present in other isoforms [18]. Sequence fidelity of the EF hand domains is crucial for the ability of the enzyme to initiate timely $[\text{Ca}^{2+}]_i$ oscillations within the oocyte [19], and EF3 is responsible for a 100-fold higher Ca^{2+} sensitivity to PIP_2 hydrolysis as compared to other PLC isoforms [20, 21]. Moreover, point mutations in the X catalytic domain of the PLCZ sequence are sufficient to abrogate its intracellular Ca^{2+} -releasing activity [19]. Therefore, species-specific differences in PLCZ sequence may be at least partially responsible for the variations in activity and pattern of $[\text{Ca}^{2+}]_i$ responses observed at fertilization for the different mammalian species studied [8, 13]. For instance, human PLCZ has an approximately 2- to 10-fold higher potency than the simian and mouse counterparts, respectively, in its ability to induce $[\text{Ca}^{2+}]_i$ oscillations in mouse oocytes [13, 22]. In addition, recent research suggests that the linker region between the X and Y catalytic subunits of the PLCZ protein has important regulatory functions regarding its specific enzymatic activity [19, 23]; interestingly, this is the least-conserved region of the protein among mammalian species in which PLCZ has been sequenced.

Species-specific differences are also manifested at the level of PLCZ expression and localization in sperm. For instance, PLCZ is immunolocalized to the equatorial region of bull sperm [24] and to the acrosomal and postacrosomal regions of

¹Supported by the Harry M. Zweig Memorial Fund for Equine Research and by start-up funds at Cornell University, College of Veterinary Medicine.

²Correspondence: Sylvia J. Bedford-Guaus, Department of Clinical Sciences, College of Veterinary Medicine, Cornell University, T7002 E VRT, Box 34, Ithaca, NY 14853. FAX: 607 253 3531; e-mail: sjb55@cornell.edu

Received: 31 October 2010.

First decision: 24 November 2010.

Accepted: 22 February 2011.

© 2011 by the Society for the Study of Reproduction, Inc.

eISSN: 1529-7268 <http://www.biolreprod.org>

ISSN: 0006-3363

mouse and hamster sperm [17]. Conversely, the majority of human sperm express PLCZ exclusively in the equatorial region, whereas a subpopulation of sperm also shows immunoreactivity over the acrosomal and postacrosomal regions [25]. It is plausible that species variations reflect differences in relative quantity of expression and/or additional functions of PLCZ in sperm physiology. Whereas these assumptions require further investigation, these localizations correspond to regions of the sperm that would facilitate rapid release of PLCZ upon fusion with the oocyte at fertilization.

The sequence and expression pattern of equine PLCZ has not been characterized, but indirect evidence supports the notion that horse sperm possess higher intracellular Ca^{2+} -releasing activity than mouse sperm based on the high frequency of $[\text{Ca}^{2+}]_i$ oscillations observed when injecting horse sperm into mouse oocytes [26]. Additionally, whereas microinjection of 0.5 $\mu\text{g}/\mu\text{l}$ of murine *Plcz* cRNA into mare oocytes yielded a pattern of $[\text{Ca}^{2+}]_i$ oscillations similar to that triggered by a single horse sperm, it was unable to support high rates of development to the blastocyst stage (3%–15%) [7, 27]. Previous studies corroborate the notions that the fidelity of the pattern of $[\text{Ca}^{2+}]_i$ oscillations at fertilization is an important determinant of embryonic development of oocytes [28] and that concentrations of PLCZ cRNA must be optimized to support later stages of in vitro embryonic development [22]. Nonetheless, this also raises the question of whether differences in PLCZ sequence and expression among species may determine the ability of the construct to support later stages of embryonic development. Based upon these premises, the purpose of our study was to clone the sequence of equine PLCZ as well as characterize the expression and localization pattern of catalytically active PLCZ in equine testis and sperm.

MATERIALS AND METHODS

Animals

The use of animals for the present study was performed in compliance with protocols approved by the Institutional Animal Care and Use Committee at Cornell University, College of Veterinary Medicine.

Chemicals and Reagents

Four-Bromo-Calcium Ionophore A23187 was obtained from Calbiochem. Tween 20 was purchased from Bio-Rad. Anti-PLCZ polyclonal antibody, raised in rabbit against the 19-mer sequence (MENKWFSLMVRDDFKGGKI) at the N-terminus of porcine PCLZ (NT-PLCZ), was generously donated by Dr. Rafael Fissore (Department of Veterinary and Animal Sciences, University of Massachusetts, Amherst, MA). PNA-Alexa 488, Hoechst 33258, and Alexa Fluor 555 goat anti-rabbit immunoglobulin (Ig) G were purchased from Invitrogen Corp. Vectashield was purchased from Fisher, Inc. All other chemicals were purchased from Sigma-Aldrich Chemical Company unless otherwise stated.

Molecular Cloning and Sequencing

Fresh testis tissue was obtained from a 23-year-old stallion of proven fertility. Sections of testicular parenchyma were dissected out and either snap-frozen for later use or freshly homogenized for RNA isolation with TRIzol (Invitrogen) following the manufacturer's instructions. One microgram of RNA was subjected to cDNA synthesis reactions using random hexamers from the Cloned AMV First-Strand cDNA Synthesis Kit (Invitrogen), followed by the optional step of RNA denaturation. Complementary DNA was then used as a template for PCR using Platinum Taq DNA Polymerase High Fidelity (Invitrogen) with the following profile: one cycle at 94°C for 30 sec; 30 cycles at 94°C for 30 sec, 52°C for 30 sec, and 72°C for 2 min; and one cycle at 72°C for 7 min. Specific oligonucleotide primers, 5'-TAAGCAAGGAGAAA CAGAACAGCAG-3' and 5'-CTATCTGACGTACCAAACGT-3' (IDT, Inc.), were designed with reference to the bovine PLCZ sequence (GenBank accession no. NM_001011680). Products were separated by electrophoresis on a 1% agarose gel stained with ethidium bromide. The PCR products were extracted and purified using the QIAquick Gel Extraction Kit (Qiagen) and

processed using an A-Addition Kit (Qiagen) to modify the blunt-end PCR products before being subcloned into the pGEM-T Easy Vector System I (Promega). Nucleotide sequencing confirmed the equine PLCZ clone. The equine PLCZ clone was compared to PLCZ cDNA from bovine, porcine, and human, as well as to *Plcz* cDNA from mouse, using MegAlign from the LaserGene package (DNASTAR, Inc.). The equine PLCZ clone was then subcloned into pKH3 plasmid vector containing three HA epitopes cloned upstream of the PLCZ clone. Cloning into this vector facilitated the detection of the PLCZ protein using a commercially available monoclonal antibody against the HA epitope (Roche Applied Science).

In Vitro Protein and cRNA Synthesis

To confirm the size and integrity of the translated gene product, the equine PLCZ cDNA was used as a template in a coupled transcription/translation system using reticulocyte lysates (TnT Coupled Reticulocyte Lysate System; Promega). In some studies, [^{35}S]methionine was incorporated into the synthesis reaction to radiolabel the nascent protein. In these studies, ^{35}S -labeled proteins (PLCZ and control luciferase proteins) were resolved by SDS-PAGE, and the gels were fixed in 10% acetic acid/methanol. The gels were then washed extensively in distilled water, followed by 20% isopropanol. The gels were then dried, and protein bands were visualized using autoradiography. In other experiments, unlabeled proteins were generated in vitro and incorporated into Western blot analysis using the NT-PLCZ or a mouse monoclonal antibody against the HA epitope, as detailed below.

For microinjection purposes, equine PLCZ and murine *Plcz* cDNA were transcribed in vitro using the Sp6 mMESSAGE mMACHINE kit (Ambion). The murine *Plcz* plasmid was kindly provided by Dr. Rafael Fissore. The equine PLCZ cDNA was cloned in a manner identical to that used for the mouse sequence. The cRNA was purified via the MEGAclear kit (Ambion) and NucAway spin columns (Ambion). Concentration of cRNA products was determined spectrophotometrically, and cRNA was stored at -80°C in single aliquots at a concentration of 1 $\mu\text{g}/\mu\text{l}$ until use.

Semen Collection and Preparation

Semen was collected with an artificial vagina from six adult (age, 9–23 yr) stallions of proven fertility. The sperm-rich fraction was diluted 2:1 (vol:vol) in prewarmed modified Whitten medium (MW) [29] and washed as previously described [30]. Resulting sperm suspensions were then diluted in MW to a final volume of 10×10^6 sperm/ml for capacitation experiments or in PBS at various concentrations for immediate immunoblotting or immunofluorescence experiments (see below).

For experiments requiring separation of sperm heads and tails, washed ejaculates were resuspended in PBS with the addition of a protease inhibitor cocktail and sonicated on ice five times for 2 sec each at 30% amplitude (Sonic Dismembrator 500; Fisher). For immunoblotting, heads and tails were then separated by sequential centrifugation (two times, $100 \times g$, 20 min). A suspension of pure tails was obtained from the supernatant after the first centrifugation. The second centrifugation yielded a pellet composed of almost exclusively heads, with less than 1% intact sperm.

For experiments requiring epididymal sperm, the epididymides from three stallions (age, 1–5 yr) were obtained via routine castrations performed at the Cornell University Hospital; the testes from one stallion (age, 23 yr) were obtained postmortem. Epididymides were transported to the laboratory (transport time, <5 min) in warm PBS. Each epididymal tail was dissected into small pieces and placed into 6 ml of 37°C MW for 10 min to allow sperm swim out. Sperm suspensions were washed as described above before processing for immunofluorescence.

Sperm Capacitation and Induction of Acrosomal Exocytosis

For experiments comparing PLCZ immunolocalization in noncapacitated versus capacitated sperm, the sperm collected from three stallions (age, 8–12 yr) were incubated in MW without (noncapacitating) or with (capacitating) the addition of 25 mM NaHCO_3 and 7 mg/ml of bovine serum albumin (BSA; 6 h, 37°C, humidified air) as previously described [30].

To compare the localization of PLCZ before and after acrosomal exocytosis, subsamples of sperm incubated in capacitating conditions were challenged with 5 μM calcium ionophore A23187 for induction of acrosomal exocytosis [30] and processed for immunofluorescence.

SDS-PAGE and Immunoblotting

For identification of PLCZ in fresh sperm samples, sperm, after initial washing, were resuspended in PBS, counted, and aliquoted to final sperm

numbers ranging from 0.05 to 10×10^6 sperm; 1×10^6 sperm were used for positive control against recombinant PLCZ. Samples were processed for SDS-PAGE and immunoblotting as previously described [30]. For immunodetection, incubation in anti-NT-PLCZ (1:1000 in 5% skim milk) or anti-HA (1:1000 in 5% skim milk) antibodies (overnight at 4°C) was followed by incubation in goat anti-rabbit horseradish peroxidase (HRP)-coupled IgG secondary antibody (1:5000 in TBS-Tween 20, 1 h, room temperature). Immunoreactivity was visualized using enhanced chemiluminescence detection with an ECL kit (Amersham Corp.) according to the manufacturer's directions.

Immunofluorescence

Immunofluorescence for localization of PLCZ was performed in epididymal (caput, corpus, and cauda), freshly ejaculated, capacitated, and acrosome-reacted sperm. After initial preparation, sperm were washed with PBS by centrifugation ($500 \times g$, 8 min). The supernatant was discarded, the pellet diluted in fresh PBS, and sperm counted using a hemocytometer. An aliquot was then diluted in PBS at 3×10^6 sperm/ml, and 125 μ l from this suspension were pipetted onto 0.1% poly-L-lysine-coated slides and allowed to settle for 15 min. Sperm were fixed with 3.7% paraformaldehyde for 30 min at 4°C, gently washed three times with 1 ml of PBS, and permeabilized with 0.1% Triton X-100 in PBS for 10 min at room temperature. After gentle washing, sperm were blocked in 5% BSA at 4°C in a humidified chamber overnight. The NT-PLCZ antibody (1:100 in blocking buffer) was added to the sperm and again incubated overnight at 4°C in a humidified chamber. Negative controls included incubating sperm with either 5 mg/ml of rabbit IgG (in blocking buffer) or antigenic blocked peptide (30 μ g of NT-PLCZ peptide preincubated for 2 h with anti-PLCZ antibody in wash buffer) in place of the primary antibody overnight at 4°C in a humidified chamber. Sperm were then washed three times with 1 ml of 0.1% Tween 20 in PBS and incubated with Alexa Fluor 555 goat anti-rabbit IgG secondary antibody (1:200 in blocking buffer) for 1 h at room temperature in the dark. Peanut agglutinin-lectin Alexa Fluor 488 HRP conjugate at 20 μ g/ml was then added for an additional 1 h, followed by incubation with Hoechst 33258 at 5 μ g/ml for 10 min at room temperature in the dark. Slides were washed (0.1% Tween 20 in PBS) and mounted with Vectashield (Vector Laboratories). The next day, slides were analyzed for the pattern of PLCZ localization using an upright fluorescent Zeiss Imager ZI microscope (Carl Zeiss, Inc.) with green fluorescent protein, DAPI, and Texas red filters.

Immunohistochemistry

Fresh testis tissue from three stallions (same group used for PLCZ immunolocalization in epididymal sperm) was obtained via routine castrations (age, 1 and 3 yr) or postmortem (age, 23 yr) at the Cornell University Hospital. Testes were transported to the laboratory (transport time, <5 min) in warm PBS. Tissue samples were fixed in 4% paraformaldehyde for 24 h before being dehydrated in increasing concentrations of ethanol (30%, 60%, 90%, and 100%). The tissue was then sent to the Cornell University Histology Laboratory in 70% ethanol, embedded in paraffin, and sectioned in chronological order on poly-L-lysine-coated slides. The slides were deparaffinized with xylene, rehydrated with decreasing concentrations of ethanol washes, and then blocked with 0.5% H_2O_2 in methanol for 10 min. Antigen retrieval was performed using a Zymed kit with ethylenediaminetetra-acetic acid (EDTA) solution (pH 8.0) for heat-induced epitope retrieval (Invitrogen) according to the manufacturer's directions. Briefly, the slides were steamed in $1 \times$ EDTA for 5 min in a microwave on high (800 W) and then for 15 min on medium (320 W). Slides were washed with 0.05% Tween 20 in 0.01 M PBS, permeabilized in 0.05% Triton X-100 in 0.01 M PBS for 5 min, and blocked in 10% goat serum with $2 \times$ casein (Vector Laboratories) for 20 min at room temperature. Incubation with NT-PLCZ was then performed at a 1:100 dilution in PBS with $1 \times$ casein for 1.5 h at 37°C. For negative controls, slides were incubated in antigenic peptide-blocked NT-PLCZ antibody (as described above) for 1.5 h at 37°C. Slides were then incubated in biotinylated goat anti-rabbit IgG secondary antibody (Vector Laboratories) for 20 min (23–25°C) at a 1:200 dilution in PBS. Next, the slides were washed with PBS and incubated in streptavidin peroxidase (Invitrogen) for 20 min (23–25°C). Visualization of PLCZ localization was achieved using the Aminoethyl Carbazole Substrate Kit (Invitrogen) for approximately 10 min according to the manufacturer's directions. The tissue sections were then counterstained with Gills #2 Hematoxylin (Fisher) for 15 sec at room temperature and mounted with an aqueous mounting medium.

Preparation of Spermatogenic Cell Suspension

Testis tissue from a mature (age, 6 yr) stallion of proven fertility was used to separate spermatogenic cell suspensions following the method described by Joshi et al. [31]. Briefly, small pieces (six pieces, each 5 mm in diameter) of cut testicular parenchyma were placed in 50 ml of BioWhittaker Minimum

Essential Medium Eagle (EMEM; Fisher) supplemented with 2 mg/ml of collagenase in an Erlenmeyer flask. The flask was placed in a 33°C automated water bath shaking at 130 rpm for approximately 1 h, until dissociation of the seminiferous tubules could be visually observed. The solid suspension of cells was then allowed to settle by gravity and the fluid decanted. In this manner, the suspension was washed three times with 50 ml of EMEM. After the last wash, 0.5 mg/ml of trypsin and 100 μ l/ml of DNase I were added, and the flask was returned to the shaking water bath for 15 min. The reaction was then stopped with 0.5 mg/ml of soybean trypsin inhibitor. Next, the suspension was gently pipetted with a large bore (4 mm) plastic pipette to break up any remaining small clumps of tissue and then filtered through an 80- μ m nylon screen. The suspension was then centrifuged twice at $450 \times g$ for 10 min, and the pellet was resuspended with wash buffer (EMEM containing 0.25 mg/ml of soybean trypsin inhibitor and 0.5 μ g/ml of DNase); the final 20 ml of resuspended cells were kept at 5°C overnight for the first set of injections. Aliquots of cells were also resuspended in 1 ml of 10% dimethyl sulfoxide in EMEM (vol:vol) solution in Eppendorf tubes and snap-frozen by plunging them in liquid nitrogen, with subsequent storage at -196°C . These cells were used in subsequent experiments whereby aliquots were thawed slowly at room temperature, washed twice in EMEM plus 0.5% (wt:vol) BSA, and checked for viability by eosin staining before injection into mouse oocytes.

Preparation of Mouse Oocytes

B6D2F1 or CD1 female mice (Harlan Sprague Dawley, Inc.) were superovulated by injections with 5 IU of equine chorionic gonadotropin (formerly PMSG), followed by injection of 5 IU of human chorionic gonadotropin (hCG) 48 h later (EMD Serono, Inc.). Oocytes were collected 13–14 h after hCG injection, placed into Hepes-buffered tyrode-lactate solution (TL-Hepes) [32] supplemented with 10% fetal calf serum (vol:vol), and denuded in 0.1% porcine hyaluronidase in PBS (wt:vol). Denuded oocytes were then placed into fresh TL-Hepes with 1 μ mol/L of Fura 2-acetoxymethylester (Fura 2-AM; Molecular Probes) supplemented with 0.02% pluronic acid (Molecular Probes) at 37°C for 20 min. After Fura 2-AM loading, oocytes were placed in warm TL-Hepes and kept at 37°C until micromanipulation.

Oocyte Microinjection

Fura 2-AM-loaded mouse (CD1) oocytes were microinjected under an inverted Eclipse TE-200 microscope (Nikon, Inc.) using an Eppendorf Transferman NK-2 (Brinkman Instruments, Inc.) micromanipulators and an Eppendorf Femtojet microinjector (Brinkman Instruments, Inc.). The injection pipette containing medium (control) or 1 μ g/ μ l of equine or murine PLCZ cRNA was advanced into the cytoplasm of each oocyte for microinjection (~ 10 pl).

Intracytoplasmic Sperm Injection or Round Spermatid Injection

Intracytoplasmic sperm injection (ICSI) or round spermatid injection (ROSI) was performed on MII mouse oocytes (B6D2F1) using sperm heads and tails from two different proven stallions (age, 9 and 18 yr) or round spermatids from a proven stallion (age, 6 yr) that was castrated at the Cornell Hospital for Animals. Injections of sperm or round spermatids were performed using Eppendorf Transferman NK-2 micromanipulators with a piezomicropipette-driving unit (Prime Tech Piezo Impact Drill PMM-150FU; Eppendorf) as previously described [7]. Mock injections were performed by injecting fluid from the sperm head/tail or round cell suspension, which served as a negative control; care was taken that the amount of fluid injected was similar to that injected with an individual sperm head, tail, or round cell. Worth noting is that the injection pipette used had only 6 μ m of internal diameter. Therefore, incorporation of a round spermatid within the pipette resulted in its complete disintegration. However, care was taken to inject all components of the cell, which tended to stick together.

Fluorescence Recordings and $[Ca^{2+}]_i$ Determination

The $[Ca^{2+}]_i$ monitoring was carried out with Fura 2-AM-loaded mouse oocytes after microinjection or ICSI/ROSI as previously described [27]. At least three replicates per experiment were performed. Recording of 340:380 nm fluorescence ratios, which correlate to $[Ca^{2+}]_i$, was performed for 1–2 h.

Statistical Analyses

Data for $[Ca^{2+}]_i$ oscillations (Tables 1 and 2) were compared by one-way ANOVA using SigmaStat software. Differences were considered to be significant at $P < 0.05$.

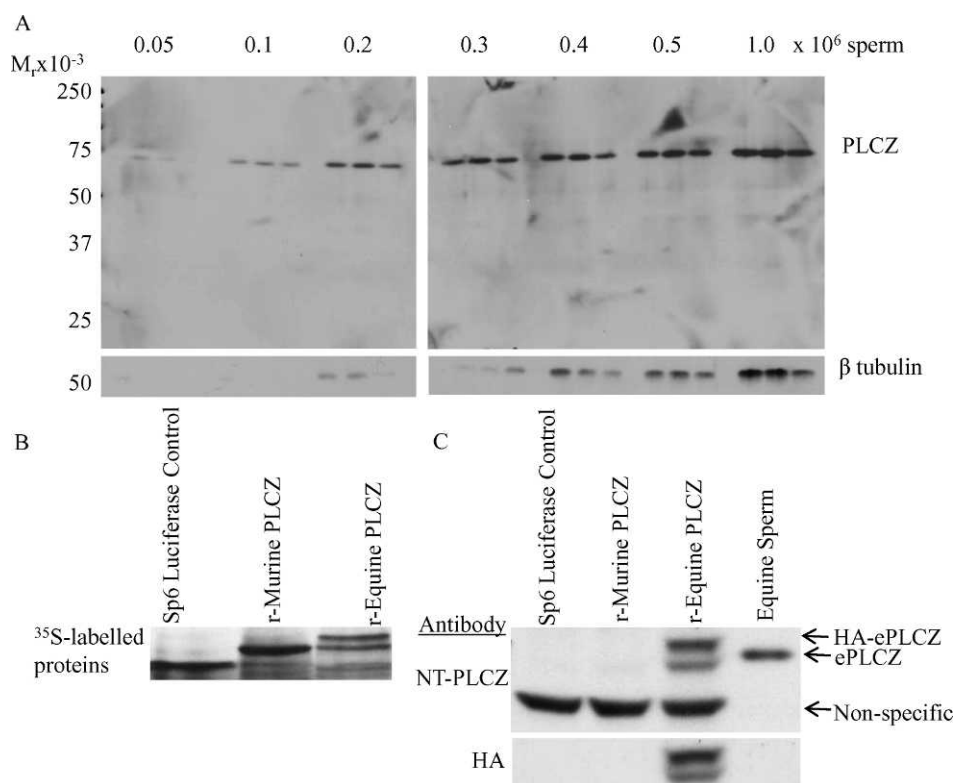


FIG. 1. **A)** PLCZ immunoblotting for different concentrations of sperm from three stallions of proven fertility. Increasing the number of sperm results in a corresponding relative increase in PLCZ immunoreactivity. The blot was reprobed with anti- β -tubulin antibody to control for protein load. **B)** Autoradiograph of ^{35}S -labeled equine recombinant PLCZ protein. **C)** Immunoblot for equine PLCZ recombinant protein using antibodies against NT-PLCZ and an HA epitope. Note that NT-PLCZ does not recognize the murine protein.

RESULTS

Identification and Molecular Cloning of Equine PLCZ

We first determined that immunoblotting of equine sperm using an antibody raised against the N-terminus of the porcine sequence yielded a specific band of the expected molecular size (~ 73 kDa) (Fig. 1A), consistent with the expression of equine PLCZ. Interestingly, at levels of sperm for which tubulin was beneath the detectable level of the assay, we could easily observe PLCZ immunoreactivity, potentially suggesting a relative high abundance of the latter in stallion sperm.

The cDNA sequence encoding equine PLCZ yielded a single open-reading frame of 1914 bp encoding for a 638-amino-acid protein (Fig. 2), with a predicted molecular size of approximately 73 kDa. Multiple ClustalW alignments of the predicted equine amino acid sequence with bovine, porcine, human, and murine PLCZ revealed 79.4%, 82.5%, 82.1%, and 71.9% homology, respectively (Fig. 3). As suspected, the X-Y linker region (Fig. 2, boxed region) displayed the least regional homology among different species.

In addition, multiple ClustalW sequence alignments with murine and human PLC delta4 (*PLCD4*; data not shown) also revealed that equine PLCZ lacks the PH domain found at the N-terminus of other PLC isoforms, as previously shown in other mammalian species for this isoform [8, 13, 15] (for review, see [33]). However, the typical X and Y, C2, and EF hand domains are conserved, as reported for PLCZ in other species (Fig. 2).

From the cloned sequence, recombinant PLCZ protein was generated using a [^{35}S]methionine reticulocyte lysate transcription/translation system. Gel analysis revealed protein bands at approximately 73 kDa for equine and for murine (control) extracts (Fig. 1B). Moreover, protein resulting from an HA-tagged PLCZ sequence was recognized both by antibodies against the HA epitope as well as by the NT-PLCZ antibody (Fig. 1C). Noteworthy is that this anti-PLCZ antibody does not

recognize the murine product. These results support the notion that the sequence cloned herein encodes for equine PLCZ.

Equine PLCZ cRNA Induces $[\text{Ca}^{2+}]_i$ Oscillations in Mouse Oocytes

To test the catalytic activity of the equine PLCZ clone, 1 $\mu\text{g}/\mu\text{l}$ of cRNA was microinjected into mouse oocytes for $[\text{Ca}^{2+}]_i$ monitoring. The same concentration of murine *Plcz* cRNA was used as a positive control. As anticipated, equine PLCZ cRNA triggered much higher relative intracellular Ca^{2+} -releasing activity than murine *Plcz* cRNA, as manifested by a higher frequency of $[\text{Ca}^{2+}]_i$ transients (Fig. 4 and Table 1).

PLCZ Localization in Equine Sperm

Previous studies have shown species-specific differences in the immunolocalization of PLCZ in sperm [17, 24, 25]. Moreover, in some species, PLCZ may undergo redistribution during sperm capacitation and the acrosome reaction [17, 25]. Therefore, we investigated the immunolocalization of PLCZ in all epididymal (head, corpus, and caput), ejaculated, capacitated, and acrosome-reacted stallion sperm. In freshly ejaculated sperm, PLCZ localized to the head region overlying the acrosome, equatorial segment, connecting piece between the head and midpiece, and most interestingly, the principal piece of the flagellum (Fig. 5A). This localization was specific, because immunoreactivity was not observed in any of these regions in the corresponding control samples (Fig. 5, D–I). Remarkably, both epididymal and capacitated sperm showed the same pattern of localization as ejaculated sperm (data not shown). However, induction of acrosomal exocytosis did result in loss of PLCZ immunofluorescence over the acrosomal region (Fig. 6A). These results raise the question of whether PLCZ may play a role in acrosomal exocytosis, as others have suggested [17, 25].

FIG. 2. Molecular cloning of equine *PLCZ*. ClustalW alignment of the predicted peptide sequence of equine with bovine (NP_0010116), porcine (NP_999515), human (NP_14911), and murine (NP_47340) *PLCZ* is shown. Upper row lists the most frequent amino acid encountered in the different species compared; X denotes that a particular amino acid is different in all species compared. A region underlined with a continuous line corresponds to the X catalytic domain. A boxed region corresponds to the X-Y linker domain. A region underlined with a broken line corresponds to the Y catalytic domain. EF hand and C2 domains correspond to unmarked N- and C-terminus regions, respectively.

	ME-----NKWFMSMRDFFRGKKINLEKTKLLEKLDIXCNXIHVKXIFKDNDRLKQGRITIEEFRTYIRIIXHREE	
	10 20 30 40 50 60 70 80	
Bovine	ME-----NKWFLLMVRDFFGKKITILEKALKLEKLDIQCNTHVKYIFKDNDRLKQGRITIEEFRTYIRIITYREE	72
Porcine	ME-----NKWFMSMRDFFGKKINLEKAKLLEKLDIQCNTHVKCI FKDNDRLKQGRITIEEFRTYIRIAHREE	72
Human	ME-----MRWFLSKIQDDFRGKKINLEKTKRLEKLDIRCSYIHVKQIFKDNDRLKQGRITIEEFRAIYRIITHREE	72
Mouse	ME-----MRWFLSKIQDDFRGKKINLEKTKRLEKLDIRCSYIHVKQIFKDNDRQKQGRITIEEFRAIYRIVHREE	80
Equine	ME-----NKWFMSMRDFFRGKKINLEKTKLLEKLDIXCNXIHVKXIFKDNDRLKQGRITIEEFRTYIRIIXHREE	72
	IIIEFNTYSENRRKILLEKNLXXFLTQEQYSLEKNXSIASEIIQKYEPPIEEVKQAHQMSXEGFTRYMDSSECLLFNXXCXX	
	90 100 110 120 130 140 150 160	
Bovine	IIIEFNTYSENRRKILLEKNLVEFLMREQYTLDFNKSIASEIIQKYEPPIEEVKQAHQMSXEGFTRYMDSSECLLFNXXCXX	152
Porcine	IIIEFNAYPENRKILFERNLIDFLTQEQYSLDINRSIVYIIQKYEPPIEEVKQAHQMSXEGFTRYMDSSECLLFNXXCXX	152
Human	IIIEFNTYSENRRKILLASNLAQFLTQEQYAAEMSKAIAFEIIQKYEPPIEEVKQAHQMSXEGFTRYMDSRECLLFNXXCXX	152
Mouse	IIIEFNTYSENRRKILLSNSLIEFLTQEQYEMIEHSDSVEIIQKYEPPIEEVKQAHQMSXEGFTRYMDSRECLLFNXXCXX	152
Equine	IIIEFNTYSENRRKILLEKNLVEFLMREQYTLDFNKSIASEIIQKYEPPIEEVKQAHQMSXEGFTRYMDSSECLLFNXXCXX	152
	VYQDMTHPLXDYFISSSHNTYLISDQLLWGPSDLWGYVSALVKGRCRLEIDCWGDSQNEPVVYHGYTLTSLKLLFKTVIQAI	
	170 180 190 200 210 220 230 240	
Bovine	VYQDMTHPLTDYFISSSHNTYLISDQLWGPSDLWGYVSALVKGRCRLEIDCWGDSQNEPVVYHGYTFTSLKLLFKTVIQAI	232
Porcine	VYQDMTHPLSDYFISSSHNTYLISDQIMGPSDLWGYVSALVKGRCRLEIDCWGDSQNEPVVYHGYTFTSLKLLFKTVIQAI	232
Human	VYQDMTHPLNDYFISSSHNTYLVSQDQLLWGPSDLWGYVSALVKGRCRLEIDCWGDSQNEPVVYHGYTFTSLKLLFKTVIQAI	232
Mouse	VYQDMNHPLSDYFISSSHNTYLISDQLWGPSDLWGYVSALVKGRCRLEIDCWGDSQNEPVVYHGYTFTSLKLLFKTVIQAI	240
Equine	TYQNMNHPLNDYFISSSHNTYLISDQLVGPSDLWGYVSALVKGRCRLEIDCWGDSQNEPVVYHGYTFTSLKLLFKTVIQAI	232
	KKYAFITSDYPPVLSLENHCSPSQEVMADNLQSTFGDALLSDXLDXFPDXLPSPEALKFKKILVRNKKIGTLKETHERGK	
	250 260 270 280 290 300 310 320	
Bovine	NKYAFITSDYPPVLSLENHCSPSQEVMADNLQSTFGDALLSDXLDXFPDXLPSPEALKFKKILVRNKKIGTLKETHERGK	312
Porcine	HKYAFITSDYPPVLSLENHCSPSQEVMADNLQSTFGDALLSDXLDXFPDXLPSPEALKFKKILVRNKKIGTLKETHERGK	312
Human	HKYAFITSDYPPVLSLENHCSPSQEVMADNLQSTFGDALLSDXLDXFPDXLPSPEALKFKKILVRNKKIGTLKETHERGK	312
Mouse	NKYAFITSDYPPVLSLENHCSPSQEVMADNLQSTFGDALLSDXLDXFPDXLPSPEALKFKKILVRNKKIGTLKETHERGK	320
Equine	RKYAFITSDYPPVLSLENHCSPSQEVMADNLQSTFGDALLSDXLDXFPDXLPSPEALKFKKILVRNKKIGTLKETHERGK	312
	XDKHGQVEEEXEEXEEXE--EDXXEVEKSEKXVDILQDXXEKEEXLKRKXVGIPLFKKKK---VKIAMALSIDLVIYTKAEKF	
	330 340 350 360 370 380 390 400	
Bovine	SDMHGKVEEEXEEXEEXE--EDGSGAKEPEPVGDFQDDLAKEEQLKRVVGIPLFRKKK---IKISMAALSIDLVIYTKAEKF	388
Porcine	FDKHGQVEEEXEEXEEXE--EEENEVRDSEILDILQDDLEKEE--LKRGVGKIFFKKKK---VKIAMALSIDLVIYTKAEKF	387
Human	SDKRGD-----NDDKQETGVKGLPGVLMFKKKTRKLLKIALALSIDLVIYTKAEKF	361
Mouse	TDKSGQVLEKWEVIYEDGD--EDSGMDPETWDVFLSRKKEERADPSLTSAGVKKR--RKMIALALSIDLVIYTKAEKF	398
Equine	TDKHGQIEEYEEVEETDQEDDDDEVKESETEDILKDNQEKEMESKRVAGLPLFKKKK---VKIAMALSIDLVIYTKAEKF	389
	RSFQHSRLYQQFNEXNSIGESQARKLSKLRASEFILHTRKFITRIYPKATRADSNNFNPQEFWNI GCMQVALNFQTPGLP	
	410 420 430 440 450 460 470 480	
Bovine	KSFHSHLYQQFNEXNSIGESQARKLTKLAAREFILHTRRFITRIYPKATRADSNNFNPQEFWNI GCMQVALNFQTPGLP	468
Porcine	RSFHYSLYQQFNEXNSIGETQARKLSKLRASEFILHTRKFITRIYPKATRADSNNFNPQEFWNI GCMQVALNFQTPGLP	467
Human	KSFQHSRLYQQFNEXNSIGETQARKLSKLRVHEPIFHTRKFITRIYPKATRADSNNFNPQEFWNI GCMQVALNFQTPGLP	441
Mouse	RNFQYSRVYQQFNEXNSIGESRARKLSKLRVHEPIFHTRKFITRIYPKATRADSNNFNPQEFWNI GCMQVALNFQTPGLP	478
Equine	RSFQHSRLYQQFNEXNSIGESQARKLSKLRASEFILHTRKFITRIYPKATRADSNNFNPQEFWNI GCMQVALNFQTPGLP	469
	MDLQNGKFLDNGGSGYILKXFLRDXKSKFNPNKAPIDSNPITLIRLISGIQLPPSX---SSSNKADLVIIEFVGPND	
	490 500 510 520 530 540 550 560	
Bovine	MDLQNGKFLDNGGSGYILKXFLRDXKSKFNPNKAPIDSNPITLIRLISGIQLPPSY---QNKADLVIIEFVGPND	544
Porcine	MDLQNGKFLDNGGSGYILKXFLRDXKSKFNPNKAPIDSNPITLIRLISGIQLPPSYH---SSSNKADLVIIEFVGPND	546
Human	MDLQNGKFLDNGGSGYILKXFLRDXKSKFNPNKAPIDSNPITLIRLISGIQLPLT---HSSNKADLVIIEFVGPND	518
Mouse	MDLQNGKFLDNGGSGYILKXFLRDXKSKFNPNKAPIDSNPITLIRLISGIQLPPSV---SSSNKADLVIIEFVGPND	555
Equine	MDLQNGKFLDNGGSGYILKXFLRDXKSKFNPNKAPIDSNPITLIRLISGIQLPPSH---SSSNKADLVIIEFVGPND	547
	QMKQQTRVYIKKNAFSPRWNETFTFIIQVPELALIRFVVENQ--GLIAGNEFLGQYTLPLVLCMNKGYRRVPLFSKMGESLEP	
	570 580 590 600 610 620 630 640	
Bovine	QMKQQSRVYIKKNAFSPRWNETFTFIIQVPELALIRFVAENQ--GLIAGNEFLGQYTLPLVLCMNKGYRRVPLFSKMGESLEP	623
Porcine	QMKQQTRVYIKKNAFSPRWNETFTFIIQVPELALIRFVVENQ--GLITGNEFLGQYTLPLVLCMNKGYRRVPLFSKMGESLEP	625
Human	QMKQQTRVYIKKNAFSPRWNETFTFIIHVPELALIRFVVEGQ--GLIAGNEFLGQYTLPLVLCMNKGYRRVPLFSKMGESLEP	597
Mouse	HVKQQTRVYIKKNAFSPRWNETFTFIIQVPELALIRFVVENQ--GLIAGNEFLGQYTLPLVLCMNKGYRRVPLFSKMGESLEP	635
Equine	DQAKHQTRVYIKKNAFSPRWNETFTFIIQVPELALIRFVVENQ--GLIAGNEFLGQYTLPLVLCMNKGYRRVPLFSKMGESLEP	626
	ASLFIYVWYIR--	
	650	
Bovine	ASLFIYVWYIR 634	
Porcine	ASLFIYVWYIR 636	
Human	ASLFIYVWYVR 608	
Mouse	SSLFIYVWFRE 647	
Equine	PASLFIYVWYV-R 638	

Because the localization of PLCZ over the sperm flagellum appears to be unique to the stallion as compared to all other species studied to date, we wanted to corroborate the specificity of our immunofluorescence results. In this regard, immunoblotting of both populations of sperm heads and tails separated by sonication revealed a band consistent with the expression of

PLCZ (Fig. 6B). Conversely, immunoreactivity was negative for the supernatant containing the sperm during sonication. This suggests that the immunoreactivity observed for sperm tails is not a product of PLCZ solubilized within the surrounding medium during sperm processing. Immunoblotting of sperm heads and tails after sonication always yielded a

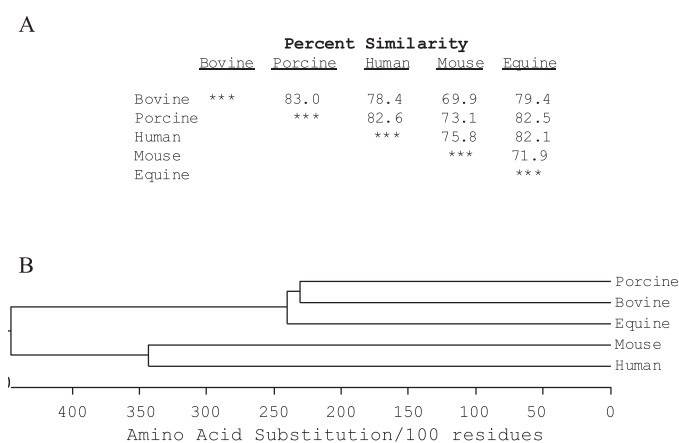


FIG. 3. **A**) Percentage homology between bovine, porcine, human, mouse, and equine PLCZ protein. **B**) Dendrogram illustrating the phylogeny of ClustalW aligned PLCZ from the same species.

series of bands assumed to be degradation products of the protein (Fig. 6B); notably, this was not observed when whole sperm were used (Fig. 1A).

Equine PLCZ Expressed over the Principal Piece of the Flagellum Is Enzymatically Active

The expression of PLCZ in regions overlying the sperm head is generally considered to be consistent with a physiological role in conferring rapid release of the enzyme at fertilization. Therefore, the finding of PLCZ expression over the principal piece of the flagellum in stallion sperm raised the question of whether this enzyme fraction is catalytically active. To test this, individual sperm heads and tails separated by sonication from a freshly collected ejaculate were injected into mouse oocytes for $[Ca^{2+}]_i$ transient monitoring. As anticipated, 8 of 10 oocytes injected with a single sperm head, and 12 of 16 oocytes injected with a single sperm tail, displayed $[Ca^{2+}]_i$ oscillations ($P > 0.05$) (Fig. 7); conversely, none of the 10 oocytes injected with the medium containing the heads and tails displayed $[Ca^{2+}]_i$ responses. In all oocytes injected with sperm heads, $[Ca^{2+}]_i$ oscillations lasted for as long as they were monitored (80–140 min); conversely, in 2 of 12 oocytes displaying $[Ca^{2+}]_i$ responses after tail injection, oscillations ceased before 1 h following injection. Analysis of the $[Ca^{2+}]_i$ oscillations detected between 20 and 30 min after ICSI revealed only a statistically significant difference in the number of spikes (Table 2). Whereas most oocytes injected with sperm tails appeared to display a lower frequency of $[Ca^{2+}]_i$ oscillations (i.e., longer interspike interval) than those injected with sperm heads, the lack of significant differences might have been caused by the great variability in $[Ca^{2+}]_i$ responses observed in oocytes

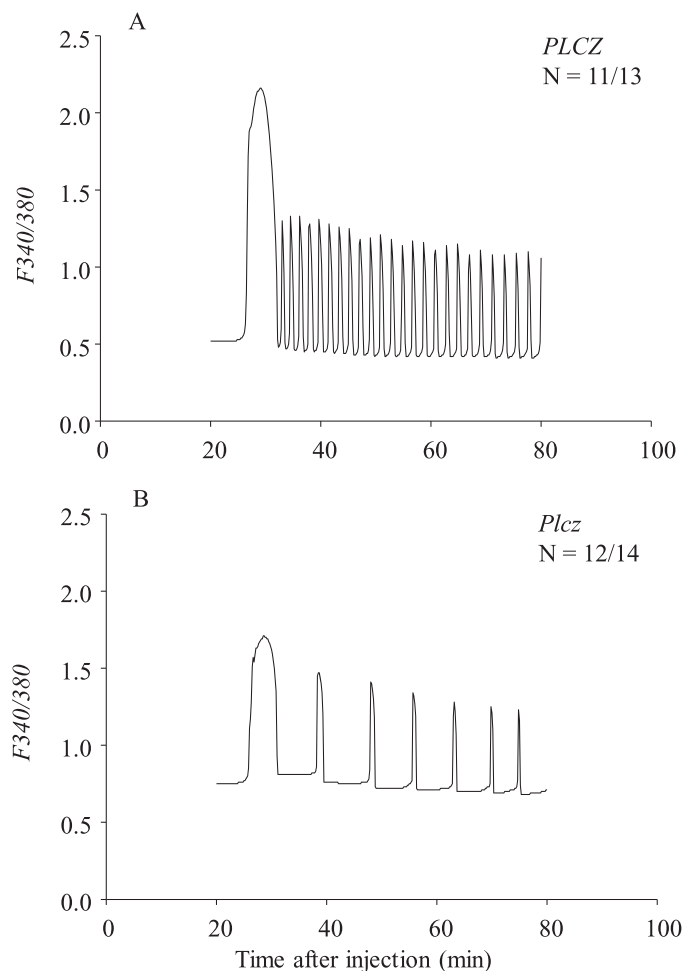


FIG. 4. Representative profiles of $[Ca^{2+}]_i$ oscillations in mouse oocytes microinjected with 1 $\mu\text{g}/\mu\text{l}$ of equine PLCZ (**A**) or murine *Plcz* (**B**) cRNA.

injected with sperm tails (Fig. 7, C and D, and Table 2). Nonetheless, the ability of the sperm flagellum to support $[Ca^{2+}]_i$ responses is an interesting and novel result and suggests potential diverse physiological functions of PLCZ in sperm.

Immunohistochemistry for PLCZ in Equine Testis Tissue

The stage of spermatogenesis at which PLCZ is first expressed has not been clearly defined. Indirect evidence suggests interspecies differences based upon injection of round spermatids into mouse oocytes and their ability (or inability) to trigger $[Ca^{2+}]_i$ oscillations and/or oocyte activation [34–39]. Immunohistochemistry was performed to characterize the ontogeny of PLCZ protein expression in equine testis tissue

TABLE 1. Characterization of $[Ca^{2+}]_i$ oscillations in mouse oocytes injected with 1 $\mu\text{g}/\mu\text{l}$ of equine or murine phospholipase C zeta cRNA (ePLCZ or mPlcz, respectively).

Treatment	No. of oocytes displaying $[Ca^{2+}]_i$ responses/ no. oocytes injected	No. of $[Ca^{2+}]_i$ spikes ^{*,†}	Interspike interval (min) ^{*,†}	$[Ca^{2+}]_i$ spike duration (min) ^{*,†}
ePLCZ	11/13	5.14 \pm 0.40 ^a	1.01 \pm 0.14	1.43 \pm 0.10
mPlcz	12/14	1.71 \pm 0.18 ^b	7.38 \pm 0.85	1.76 \pm 0.19

* Data corresponds to $[Ca^{2+}]_i$ spikes observed between 40 and 50 min after ePLCZ and mPlcz cRNA microinjection.

† Values are mean \pm SEM.

^{a,b} Different superscript letters within a column denote significant differences ($P < 0.001$).

FIG. 5. Immunofluorescence for PLCZ in stallion sperm. Primary antibody: (A–C) NT-PLCZ, (D–F) rabbit IgG control, and (G–I) NT-PLCZ preincubated in the presence of antigenic peptide. A, F, and I) Goat anti-rabbit IgG Alexa Fluor 555-bound secondary antibody shows PLCZ localization. In A, PLCZ is localized to the region overlying the acrosome (a), equatorial segment (b), head-midpiece junction (c), and principal piece of the flagellum (d). B, D, and G) Hoechst stains the sperm nuclei. C, E, and H) Alexa Fluor 488-bound peanut agglutinin (PNA) stains the sperm acrosome. Bar = 5 μ m.

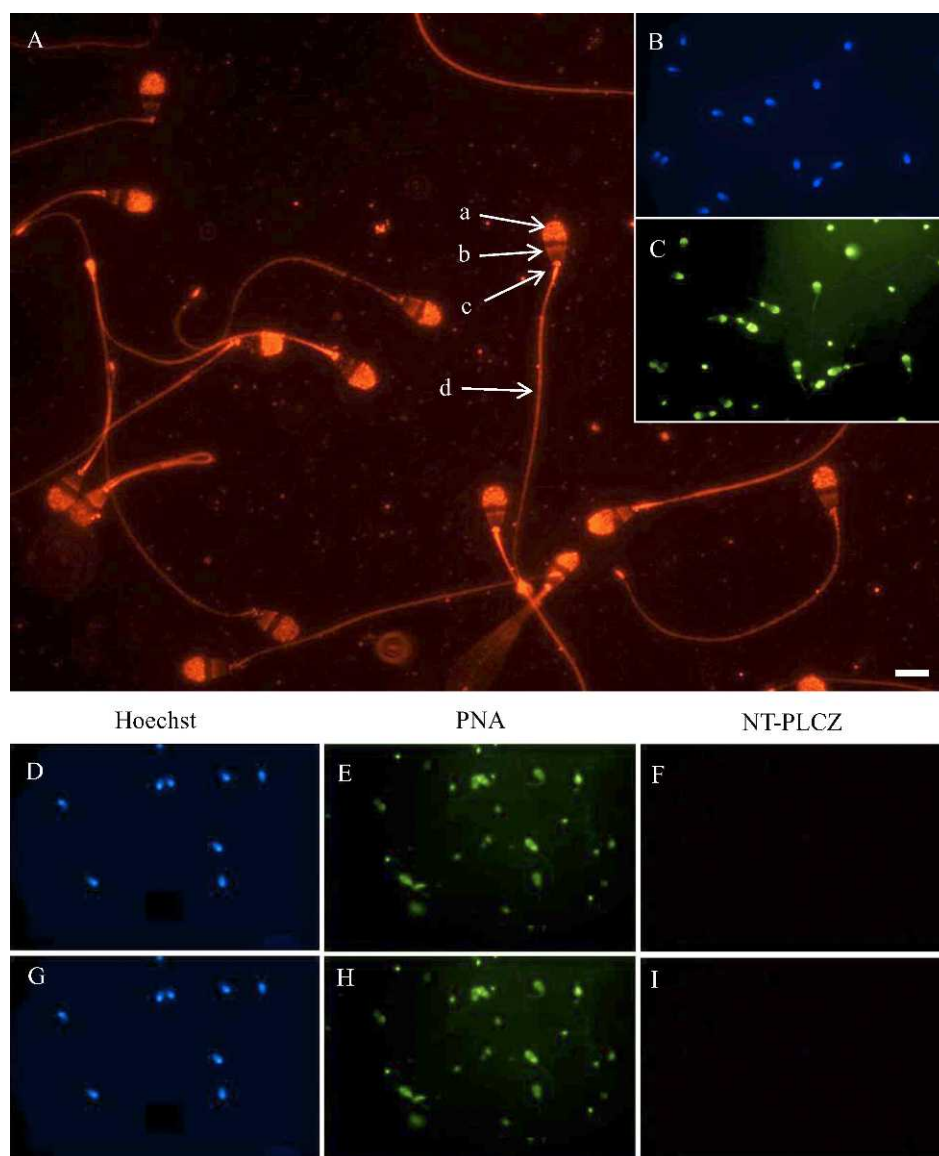


(Fig. 8). Positive staining was observed in more mature cells of the spermatogenic line, closer to the lumen of the seminiferous tubules, and thus presumed to be at the round spermatid stage (Fig. 8J). This finding was supported by the fact that PLCZ expression appeared first over a cap representing the developing acrosome. Positive staining for PLCZ was also localized to the head and tails of elongating spermatids and developing sperm (Fig. 8L), consistent with our immunofluorescence findings in mature sperm (Fig. 5). No immunostaining was observed in earlier stages of spermatogenesis (cells

closer to the basement membrane of the tubules), somatic cells, or in control samples (Fig. 8, A, C, E, G, I, and K).

Round Spermatids from Stallion Testis Express Enzymatically Active PLCZ

To ascertain whether PLCZ expressed in round spermatids (Fig. 8) is catalytically active, the cells isolated from the testis of a mature stallion of proven fertility were injected into mouse oocytes for $[Ca^{2+}]_i$ monitoring. Under phase-contrast microscopy, round spermatids were the smallest round cells observed,

TABLE 2. Characterization of $[Ca^{2+}]_i$ oscillations in mouse oocytes injected with stallion sperm heads or tails.

Sperm	No. of oocytes displaying $[Ca^{2+}]_i$ responses/no. oocytes injected	No. of $[Ca^{2+}]_i$ spikes* [†]	Interspike interval (min)* [†]	$[Ca^{2+}]_i$ spike duration (min)* [†]
Heads	8/10	6.75 \pm 0.92 ^a	0.59 \pm 0.20	1.21 \pm 0.12
Tails	12/16	3.08 \pm 0.82 ^b	1.90 \pm 0.95	2.31 \pm 0.51

* Data corresponds to $[Ca^{2+}]_i$ oscillations observed between 20 and 30 min after sperm head or tail injection.

[†] Values are mean \pm SEM.

^{a,b} Different superscript letters within a column denote significant differences ($P < 0.05$).

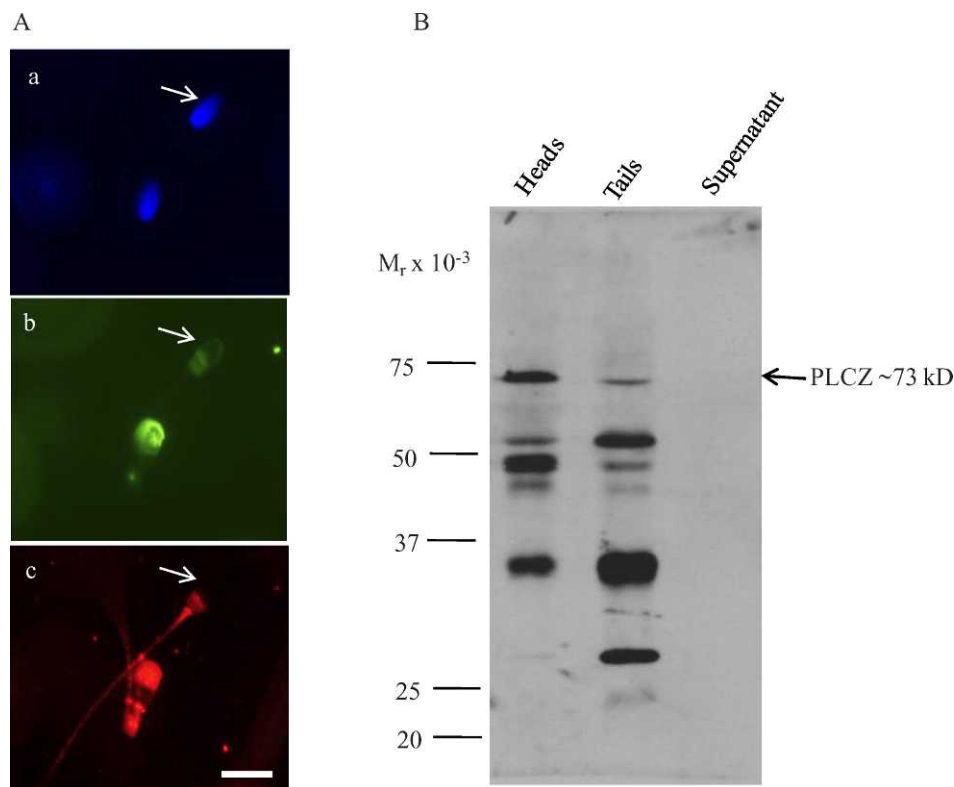


FIG. 6. **A**) Immunofluorescence for PLCZ in capacitated stallion sperm induced to undergo acrosomal exocytosis: **(a)** Hoechst stains sperm nuclei, **(b)** Alexa Fluor 488-bound peanut agglutinin (PNA) stains the sperm acrosomes, and **(c)** localization of PLCZ using NT-PLCZ primary antibody and goat anti-rabbit IgG Alexa Fluor 555-bound secondary antibody. Arrow points at acrosome-reacted sperm as denoted by the lack of PNA staining and consequent loss of PLCZ immunostaining. **B**) Immunoblotting for PLCZ in both heads and tails of stallion sperm. Stallion sperm were sonicated to detach the heads from tails and centrifuged to obtain pure populations of each. The equivalent of 1×10^6 sperm heads or tails were loaded per lane as well as the supernatant resulting from sonication. Immunoblotting shows a band at approximately 73 kDa for both head and tail populations but not the supernatant fraction. Bar = 5 μ m.

displaying an eccentric nucleus and a smooth cytoplasm (Fig. 9A). In contrast, spermatocytes were markedly larger in size, with a granular cytoplasm, and often were binucleated (Fig. 9A). In total, 6 of 10 mouse oocytes injected with round spermatids displayed $[Ca^{2+}]_i$ transients, with an interspike interval of 2.29 ± 0.54 min (mean \pm SEM) and an average spike duration of 3.14 ± 0.59 min (mean \pm SEM; Fig. 9B).

Conversely, none of the six oocytes injected with the suspending medium displayed $[Ca^{2+}]_i$ responses.

DISCUSSION

Mounting evidence supports the notion that oocyte activation at fertilization is brought about by a factor introduced by the sperm—namely, the testis-specific PLCZ

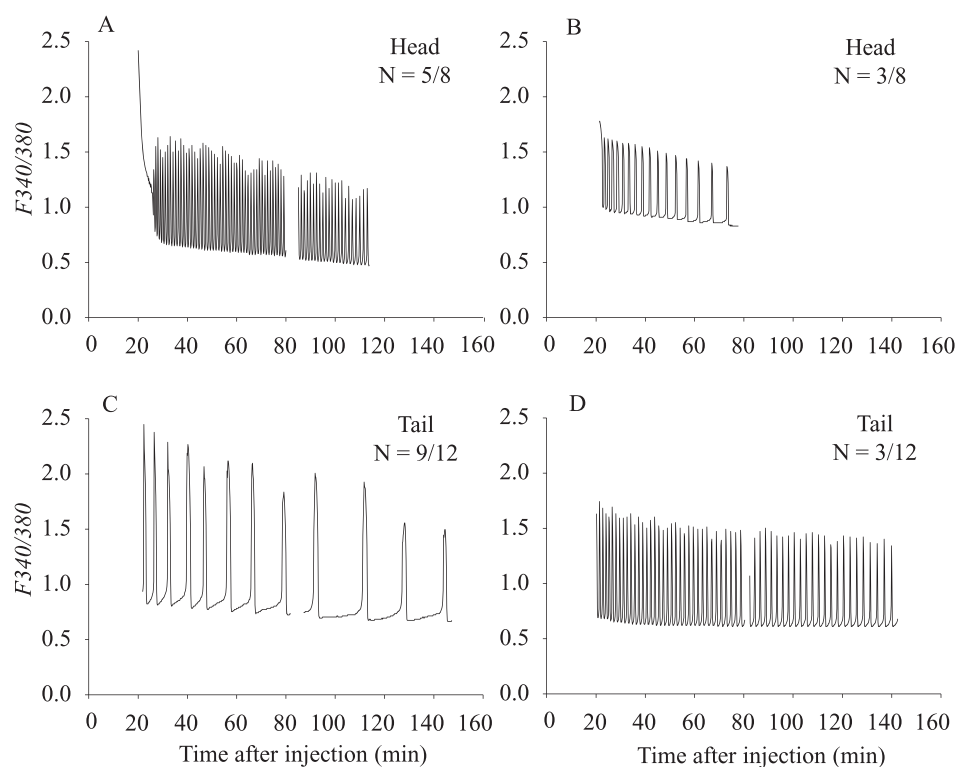


FIG. 7. Representative $[Ca^{2+}]_i$ transient profiles for mouse oocytes injected with an equine sperm head **(A and B)** or tail **(C and D)**. Both sperm heads and tails were able to induce $[Ca^{2+}]_i$ oscillations when injected into mouse oocytes. Negative controls injected with supernatant did not display $[Ca^{2+}]_i$ responses.

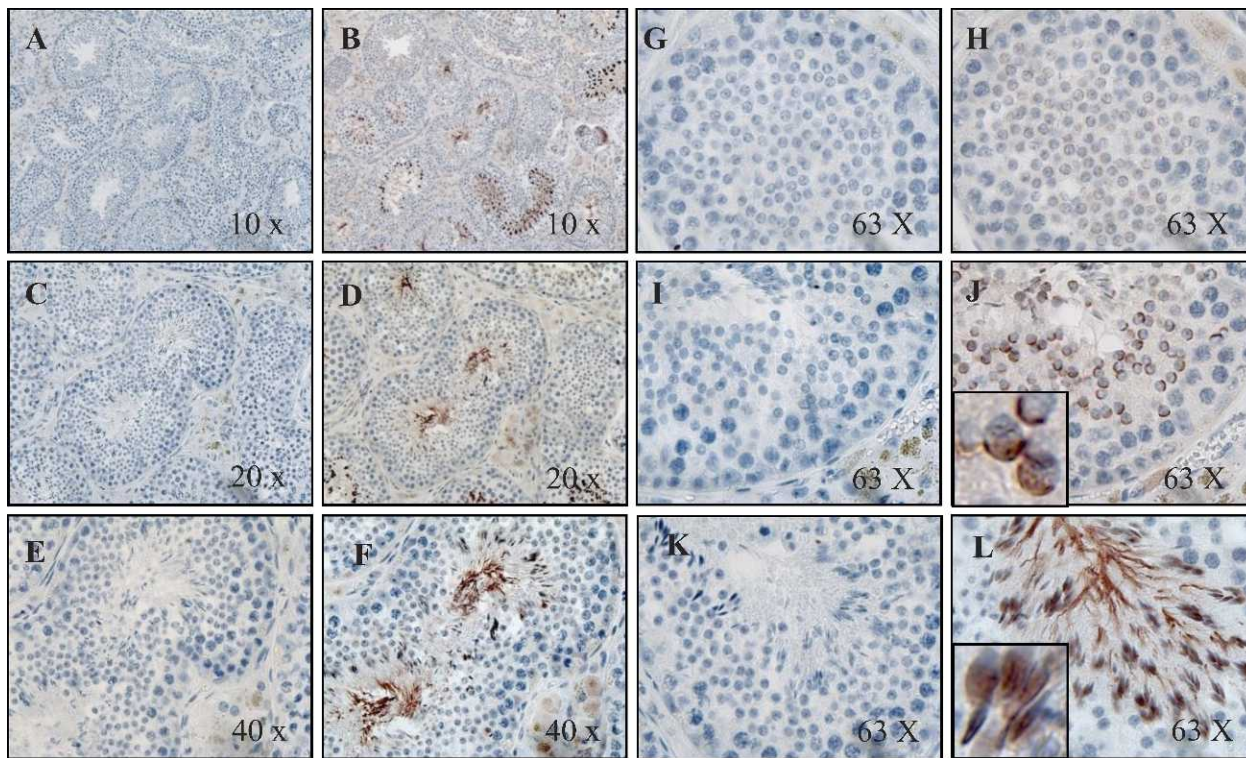


FIG. 8. Immunohistochemistry for PLCZ expression on testis tissue from a mature stallion of proven fertility. **A, C, E, G, I, and K)** N-terminus PLCZ antibody was preincubated with the corresponding antigenic peptide. **B, D, F, H, J, and L)** Equine PLCZ is expressed in developing spermatogenic cells beginning at the round spermatid stage. In **J and L**, insets show that PLCZ expression overlays the acrosome in round and elongating spermatids. In **L**, PLCZ is also expressed along the flagellum of elongating spermatids and sperm.

[8, 13–17, 40] (for review, see [33]). Whereas this appears to be a highly conserved mechanism among mammals, species-specific differences in *PLCZ* sequence, activity, and expression have been reported, thus enhancing our knowledge of the molecular mechanisms surrounding fertilization. Herein, we report the sequence and ontogeny of testicular expression and sperm immunolocalization of equine PLCZ. Notably, we show unique species-specific differences in the intrinsic activity and, in particular, in the expression of catalytically active PLCZ in sperm and testis.

The sequence of equine *PLCZ* reveals a structure similar to those of other *PLCZ* genes characterized to date, with four EF hand domain motifs, X and Y catalytic domains (separated by a linker region), and a C2 domain [8, 13, 15–17]. Similarly, sequence alignment with murine and human *PLCD4* reveals that equine *PLCZ* lacks the N-terminal PH domain typical for other PLC isoforms (data not shown). However, despite the seemingly conserved nature of *PLCZ* between different species, it appears that just small sequence differences are sufficient to markedly affect the activity of the construct in a species-specific manner [13, 41] and, potentially, its ability to support advanced stages of embryonic development. In this regard, we report that microinjection of 1 $\mu\text{g}/\mu\text{l}$ of equine *PLCZ* cRNA into mouse oocytes is able to induce a significantly higher frequency (~ 3 -fold increase) of $[\text{Ca}^{2+}]_i$ oscillations than microinjection of the same concentration of murine *Plcz* cRNA. Whereas differences in the relative expression of each of the two proteins (murine vs. equine) in mouse oocytes, which was not quantified herein, could account for these findings [16], we assume similar protein expression efficiency given that both equine *PLCZ* and mouse *Plcz* cRNA were expressed from the same vector. Moreover, because injected *PLCZ* cRNA requires transcription once injected into

oocytes, the lag time between microinjection and initiation of $[\text{Ca}^{2+}]_i$ transients is also considered to be an indicator of the intrinsic activity of expressed PLCZ [16, 19, 42]. In this regard, oscillations had started by the beginning of monitoring (i.e., by 20 min postinjection) in 7 of 11 versus 2 of 12 oocytes displaying $[\text{Ca}^{2+}]_i$ transients and injected with equine *PLCZ* or murine *Plcz* cRNA, respectively. These findings corroborate the notion that equine *PLCZ* possesses higher enzymatic activity than the murine counterpart and support our suspicions based upon the high frequency of $[\text{Ca}^{2+}]_i$ oscillations previously observed when injecting horse sperm into mouse oocytes [26]. Notably, the equine *PLCZ* clone shows highest homology with porcine (82.5%), human (82.1%), and bovine (79.4%) *PLCZ* but only a 71.9% homology with the murine protein. Interestingly, when compared to murine *Plcz* cRNA, both the human and bovine constructs also display a higher relative intracellular Ca^{2+} -releasing activity when their corresponding *PLCZ* cRNA is microinjected into mouse oocytes [16, 41].

The species-specific differences in enzymatic activity of PLCZ can probably be attributed to amino acid substitutions in different regions of the sequence. In this regard, the EF hand domains are crucial for the *in vivo* activity of the protein and for the high sensitivity to basal levels of $[\text{Ca}^{2+}]_i$ (i.e., median effective concentration = 50–80 nM) displayed by PLCZ [20, 43]. In turn, evidence also suggests that a cluster of basic amino acids in the X-Y linker region may be involved in the anchoring of PLCZ to its substrate, PIP_2 [44]. Moreover, the X-Y linker region may play an important function in the regulation of the specific enzymatic activity of the protein [19, 23]. It has been suggested that *in vivo* proteolysis on this region may determine a conformational change in the protein, thus facilitating access of the catalytic site to PIP_2 [23].

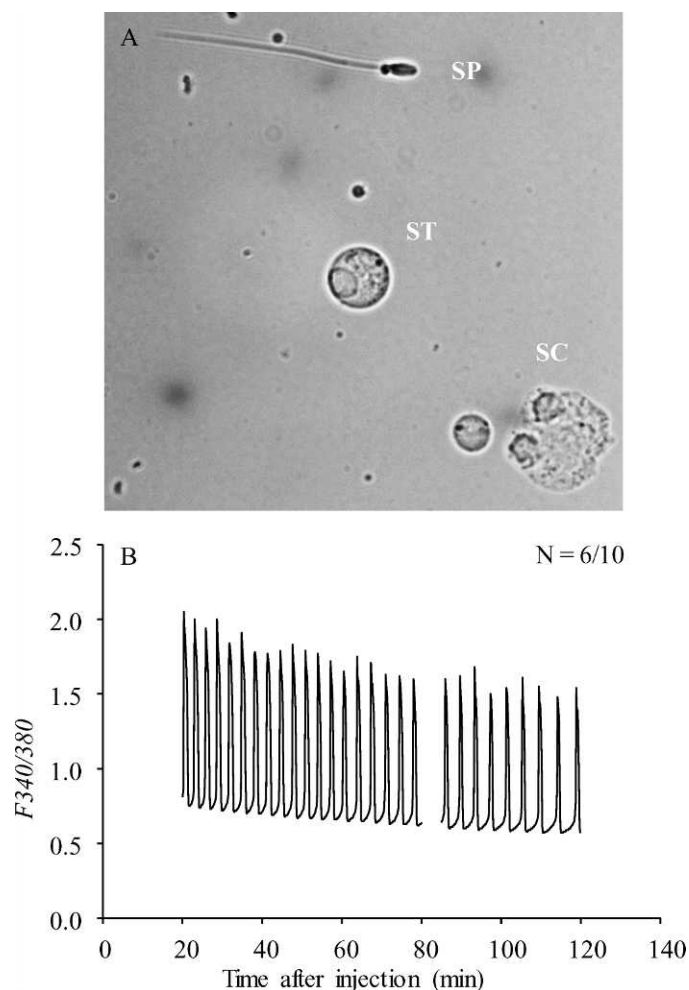


FIG. 9. Round spermatids isolated from equine testis and injected into mouse oocytes trigger $[Ca^{2+}]_i$ oscillations. **A**) Phase-contrast image showing a stallion sperm (SP), round spermatid (ST), and spermatocyte (SC) isolated from stallion testis. Original magnification $\times 400$. **B**) Representative profile of $[Ca^{2+}]_i$ oscillations displayed by a mouse oocyte injected with a round spermatid from equine testis.

Interestingly, this is the region of the protein showing most divergence among species; notably, the sequence of the X-Y linker region of equine PLCZ shows greatest similarity with that of the human, bovine, and porcine (49.0%, 48.1%, and 47.4% homology, respectively, vs. 35.4% homology with the mouse), which may account for different relative enzymatic activities displayed by their corresponding proteins.

The present study also reveals unique species-specific differences regarding the expression of PLCZ in sperm and testis. Most notably, we show via immunofluorescence and immunoblotting that PLCZ is expressed in both the head (acrosomal and equatorial regions) and the principal piece of the flagellum in equine sperm. In other species, reported discrepancies in PLCZ localization in sperm have been attributed to the particular antibody used [17, 24, 45]. Whereas we have only tested one anti-PLCZ antibody in the present study and this could account for some of our findings, the fact that injection of sperm flagella into mouse oocytes induced $[Ca^{2+}]_i$ oscillations provides direct evidence for the expression of catalytically active protein in this sperm region. To our knowledge, this has not been reported in any other species. Immunofluorescence studies have shown that PLCZ localizes to the equatorial region of bull and human sperm [24, 25] and

to the acrosomal and postacrosomal regions of mouse, hamster, and human sperm [17, 25, 45]. Moreover, whereas Fujimoto et al. [45] reported weak PLCZ immunostaining of the flagellum in mouse sperm, it was previously shown that injection of one to three mouse sperm tails failed to induce oocyte activation [46]. In addition, incubation of stallion sperm in capacitating conditions did not alter the pattern of expression of PLCZ, as has been reported for mouse and hamster sperm [17]. However, induction of acrosomal exocytosis did abrogate PLCZ immunostaining over the acrosomal region, as previously shown for all mouse, hamster, and human sperm [17, 25], suggesting that PLCZ over this sperm region does not contribute to oocyte activation. Altogether, these findings raise the possibility of potential additional physiological functions of the catalytically active PLCZ localized over the acrosome and principal piece of equine sperm.

Species-specific differences have also been noted in the ontogeny of expression of PLCZ in the testis. For instance, in the mouse, rabbit, rat, and pig, round spermatids do not yet express PLCZ [15, 34–39, 47], because the expression of the protein is first evident at the elongated spermatid stage [15, 34, 36]. Whereas in the mouse normal offspring have been produced by the injection of these round cells, an additional activation mechanism is necessary to initiate $[Ca^{2+}]_i$ rises and, thus, the embryonic development program [34, 36]. Conversely, human- and hamster-derived round spermatids are able to support $[Ca^{2+}]_i$ oscillations and, thus, activation when injected into mouse oocytes [35, 48], thereby supporting the notion that enzymatically active protein is expressed by these cells. Similarly, we show conclusive evidence of catalytically active equine PLCZ expression as early as the round spermatid stage.

In summary, we present a novel sequence for equine PLCZ, which transcribes into a product displaying high intrinsic intracellular Ca^{2+} -releasing activity in mouse oocytes. Additionally, we reveal species-specific findings regarding the expression of catalytically active PLCZ in equine sperm and testis. Further studies should be directed at more closely analyzing the specific catalytic activity of the equine clone, with special attention to the regions of the sequence that determine such activity via mutational analysis. It would also be interesting to ascertain the potential physiological relevance of PLCZ expression in the acrosome and principal piece of stallion sperm, because this may be potentially related to other important functions, such as acrosomal exocytosis and/or hyperactivation of motility. We also plan on characterizing the activity of equine PLCZ and ability to support parthenogenetic embryonic development when injected into mare oocytes.

ACKNOWLEDGMENTS

The authors thank Dr. Rafael Fissore for generously providing the murine *Plcz* plasmid and anti-PLCZ antibody used for these experiments. The authors also thank Ms. Carol Collyer, Mr. Larry Dodge, and Drs. Katherine Beltaire, Christine Schweizer, Valeria Tanco, and Robert Gilbert for their assistance with semen collection from stallions.

REFERENCES

1. Fissore RA, Gordo AC, Wu H. Activation of development in mammals: is there a role for sperm cytosolic factor? *Theriogenology* 1998; 49:43–52.
2. Kurokawa M, Sato K-I, Fissore RA. Mammalian fertilization: from sperm factor to phospholipase C ζ . *Biol Cell* 2004; 96:37–45.
3. Fissore RA, Dobrinsky JR, Balise JJ, Duby RT, Robl JM. Patterns of intracellular Ca^{2+} concentration in fertilized bovine oocytes. *Biol Reprod* 1992; 47:960–969.
4. Kline D, Kline JT. Repetitive calcium transients and the role of calcium in exocytosis and cell cycle activation in the mouse egg. *Dev Biol* 1992; 149:80–89.
5. Taylor CT, Lawrence YM, Kingsland CR, Biljan MM, Cuthbertson KSR.

- Oscillations in intracellular free calcium induced by spermatozoa in human oocytes at fertilization. *Hum Reprod* 1993; 8:2174–2179.
6. Nakada K, Mizuno J, Shiraishi K, Endo K, Miyazaki S. Initiation, persistence, and cessation of the series of intracellular Ca^{2+} responses during fertilization of bovine oocytes. *J Reprod Dev* 1995; 41:77–84.
 7. Bedford SJ, Kurokawa M, Hinrichs K, Fissore RA. Patterns of intracellular calcium oscillations in horse oocytes fertilized by intracytoplasmic sperm injection: possible explanations for the low success of this assisted reproduction technique in the horse. *Biol Reprod* 2004; 7:936–944.
 8. Saunders CM, Larman MG, Parrington J, Cox LJ, Royle J, Blayney LM, Swann K, Lai FA. PLC ζ : a sperm-specific trigger of Ca^{2+} oscillations in eggs and embryo development. *Development* 2002; 129:3533–3544.
 9. Brind S, Swann K, Carroll J. Inositol 1,4,5-trisphosphate receptors are downregulated in mouse oocytes in response to sperm or adenophostin A but not to increases in intracellular Ca^{2+} or egg activation. *Dev Biol* 2000; 223:251–265.
 10. Jellerette T, He CL, Wu H, Parys JB, Fissore RA. Down-regulation of the inositol 1,4,5-trisphosphate receptor in mouse eggs following fertilization or parthenogenetic activation. *Dev Biol* 2000; 223:238–250.
 11. Jones KT, Nixon VL. Sperm induced Ca^{2+} oscillations in mouse oocytes and eggs can be mimicked by photolysis of caged inositol 1,4,5-trisphosphate: evidence to support a continuous low level production of inositol 1,4,5-trisphosphate during mammalian fertilization. *Dev Biol* 2000; 225:1–12.
 12. Wu H, Smyth J, Luzzi V, Fukami K, Takenawa T, Black SL, Allbritton NL, Fissore RA. Sperm factor induces intracellular free calcium oscillations by stimulating the phosphoinositide pathway. *Biol Reprod* 2001; 64:1338–1349.
 13. Cox LJ, Larman MG, Saunders CM, Hashimoto K, Swann K, Lai FA. Sperm phospholipase C ζ from humans and cynomolgus monkeys triggers Ca^{2+} oscillations, activation and development of mouse oocytes. *Reproduction* 2002; 124:611–623.
 14. Coward K, Ponting CP, Chang H-Y, Hibbitt O, Savolainen P, Jones KT, Parrington J. Phospholipase C ζ , the trigger of egg activation in mammals, is present in a nonmammalian species. *Reproduction* 2005; 130:157–163.
 15. Yoneda A, Kashima M, Yoshida S, Terada K, Nakagawa S, Skamoto A, Hayakawa K, Suzuki K, Ueda J, Watanabe T. Molecular cloning, testicular postnatal expression, and oocyte-activating potential of porcine phospholipase C ζ . *Reproduction* 2006; 132:399–401.
 16. Ito M, Shikano T, Oda S, Horiguchi T, Tanimoto S, Awaji T, Mitani H, Miyazaki S. Difference in Ca^{2+} oscillation-inducing activity and nuclear translocation ability of PLCZ1, an egg-activating sperm factor candidate, between mouse, rat, human, and medaka fish. *Biol Reprod* 2008; 78:1081–1090.
 17. Young C, Grasa P, Coward K, Davis L, Parrington J. Phospholipase C zeta undergoes dynamic changes in its pattern of localization in sperm during capacitation and the acrosome reaction. *Fertil Steril* 2009; 91:2230–2242.
 18. Fukami K, Inanobe S, Kanemaru K, Nakamura Y. Phospholipase C is a key enzyme regulating intracellular calcium and modulating the phosphoinositide balance. *Prog Lipid Res* 2010; 49:429–437.
 19. Kuroda K, Ito M, Shikano T, Awaji T, Yoda A, Takeuchi H, Knoshita K, Miyazaki S. The role of the X/Y linker region and N-terminal EF-hand domain in nuclear translocation and Ca^{2+} oscillation-inducing activities of phospholipase C ζ , a mammalian egg-activating factor. *J Biol Chem* 2006; 281:27794–27805.
 20. Kouchi Z, Fukami K, Shikano T, Oda S, Nakamura Y, Takenawa T, Miyazaki S. Recombinant phospholipase C ζ has high Ca^{2+} sensitivity and induces Ca^{2+} oscillations in mouse eggs. *J Biol Chem* 2004; 279:10408–10412.
 21. Kouchi Z, Shikano T, Nakamura Y, Shirakawa H, Fukami K, Miyazaki S. The role of EF-hand domains and C2 domain in regulation of enzymatic activity of phospholipase C ζ . *J Biol Chem* 2005; 280:21015–21021.
 22. Yu Y, Saunders CM, Lai FA, Swann K. Preimplantation development of mouse oocytes activated by different levels of human phospholipase C zeta. *Hum Reprod* 2008; 23:365–373.
 23. Kurokawa M, Yoon SY, Alfandari D, Fukami K, Sato K-I, Fissore RA. Proteolytic processing of phospholipase Czeta and $[\text{Ca}^{2+}]_i$ oscillations during mammalian fertilization. *Dev Biol* 2007; 31:407–418.
 24. Yoon SY, Fissore RA. Release of phospholipase C ζ and $[\text{Ca}^{2+}]_i$ oscillation-inducing activity during mammalian fertilization. *Reproduction* 2007; 134:695–704.
 25. Grasa P, Coward K, Young C, Parrington J. The pattern of localization of the putative oocyte activation factor, phospholipase C ζ , in uncapacitated, capacitated, and ionophore-treated human spermatozoa. *Hum Reprod* 2008; 23:2513–2522.
 26. Bedford SJ, Kurokawa M, Hinrichs K, Fissore RA. Intracellular calcium oscillations and activation in horse oocytes injected with stallion sperm extracts or spermatozoa. *Reproduction* 2003; 126:488–499.
 27. Bedford-Guaus SJ, Yoon SY, Fissore RA, Choi YH, Hinrichs K. Microinjection of mouse phospholipase C zeta complementary RNA into mare oocytes induces long-lasting intracellular calcium oscillations and embryonic development. *Reprod Fertil Dev* 2008; 20:875–883.
 28. Ozil JP, Huneau D. Activation of rabbit oocytes: the impact of the Ca^{2+} signal regime on development. *Development* 2001; 128:917–928.
 29. Travis AJ, Jorgez CJ, Merdiushev T, Jones BH, Dess DM, Diaz-Cueto L, Storey BT, Kopf GS, Moss SB. Functional relationships between capacitation-dependent cell signaling and compartmentalized metabolic pathways in murine spermatozoa. *J Biol Chem* 2001; 276:7630–7636.
 30. McPartlin LA, Littell J, Mark E, Nelson JL, Travis AJ, Bedford-Guaus SJ. A defined medium supports changes consistent with capacitation in stallion sperm as evidenced by increases in protein tyrosine phosphorylation and high rates of acrosomal exocytosis. *Theriogenology* 2008; 15:639–650.
 31. Joshi MS, Anakwe OO, Gerton GL. Preparation and short-term culture of enriched populations of guinea pig spermatocytes and spermatids. *J Androl* 1990; 11:120–130.
 32. Parrish JJ, Susko-Parrish J, Winer MA, First NL. Capacitation of bovine sperm by heparin. *Biol Reprod* 1988; 38:1171–1180.
 33. Swann K, Saunders CM, Rogers NT, Lai FA. PLC ζ (zeta): a sperm protein that triggers Ca^{2+} oscillations and egg activation in mammals. *Cell Dev Biol* 2006; 17:264–273.
 34. Kimura Y, Yanagimachi R. Mouse oocytes injected with testicular spermatozoa or round spermatids can develop into normal offspring. *Development* 1995; 121:2397–2405.
 35. Yazawa H, Yanagida K, Katayose H, Hayashi S, Sato A. Comparison of oocyte activation and Ca^{2+} oscillation inducing abilities of round/elongated spermatids of mouse, hamster, rat, rabbit and human assessed by mouse oocyte activation assay. *Hum Reprod* 2000; 15:2582–2590.
 36. Yazawa H, Yanagida K, Sato A. Oocyte activation and Ca^{2+} oscillation-inducing abilities of mouse round/elongated spermatids and the developmental capacities of embryos from spermatid injection. *Hum Reprod* 2001; 16:1221–1228.
 37. Loren J, Lacham-Kaplan O. The employment of strontium to activate mouse oocytes: effects on spermatid-injection outcome. *Reproduction* 2006; 131:259–267.
 38. Hirabayashi M, Kato M, Hoshi S. Factors affecting full-term development of rat oocytes microinjected with fresh or cryopreserved round spermatids. *Exp Anim* 2008; 57:401–405.
 39. Hirabayashi M, Kato M, Kitada K, Ohnami N, Hirao M, Hoshi S. Activation regimes for full-term development of rabbit oocytes injected with round spermatids. *Mol Reprod Dev* 2009; 76:573–579.
 40. Knott JG, Kurokawa M, Fissore RA, Schultz RM, Williams CJ. Transgenic RNA interference reveals role for mouse sperm phospholipase Czeta in triggering Ca^{2+} oscillations during fertilization. *Biol Reprod* 2004; 72:992–996.
 41. Ross PJ, Beyhan Z, Iager AE, Yoon S-Y, Malcuit C, Schellander K, Fissore RA, Cibelli JB. Parthenogenetic activation of bovine oocytes using bovine and murine phospholipase C zeta. *BMC Dev Biol* 2008; 8:16–27.
 42. Yoda A, Oda S, Shikano T, Kouchi Z, Awaji T, Shirakawa H, Kinoshita K, Miyazaki S. Ca^{2+} oscillation-inducing phospholipase C zeta expressed in mouse eggs is accumulated to the pronucleus during egg activation. *Dev Biol* 2004; 268:245–257.
 43. Nomikos M, Blayney LM, Larman MG, Campbell K, Rossbach A, Saunders CM, Swann K, Lai FA. Role of phospholipase C-zeta domains in Ca^{2+} -dependent phosphatidylinositol 4,5-bisphosphate hydrolysis and cytoplasmic Ca^{2+} oscillations. *J Biol Chem* 2005; 280:31011–31018.
 44. Nomikos M, Mulgrew-Nesbitt A, Pallavi P, Mihalyne G, Zaitseva I, Swann K, Lai FA, Murray D, McLaughlin S. Binding of phosphoinositide-specific phospholipase C- ζ (PLC- ζ) to phospholipid membranes. *J Biol Chem* 2007; 282:16644–16653.
 45. Fujimoto S, Yoshida N, Fukui T, Amanai M, Isobe T, Itagaki C, Izumi T, Perry ACF. Mammalian phospholipase Czeta induces oocyte activation from the sperm perinuclear matrix. *Dev Biol* 2004; 274:370–383.
 46. Kimura Y, Yanagimachi R, Kuretake S, Bortkiewicz H, Perry ACF, Yanagimachi H. Analysis of mouse oocyte activation suggests the involvement of sperm perinuclear matrix. *Biol Reprod* 1998; 58:1407–1415.
 47. Choi JY, Lee EY, Cheong HT, Yoon BK, Bae DS, Choi DS. Effects of activation timing on the fertilization rate and early embryo development in porcine ROSI procedure. *J Assist Reprod Genet* 2004; 21:329–334.
 48. Yazawa H, Yanagida K, Sato A. Human round spermatids from azoospermic men exhibit oocyte-activation and Ca^{2+} oscillation-inducing activities. *Zygote* 2007; 15:337–346.